Computational Analysis of 2D – 4Bladed Hydrokinetic Turbine

Anurag Kumar[a], Abhishek Pandey[b*]

[a] Mechanical Engineering Department, Rama University, Kanpur, UP. India
[b] Mechanical Engineering Department, ABES EC, Ghaziabad, UP. India

***Abstract*- a free stream of river, canal and other industrial waste are can be utilized for small power generation such as micro and Pico electricity in kilowatts. This potential is still untouched and calculation of complete potential is under investigation. However, technologies to tap this potential are available to validate for commercialization and prototype testing it. There is a need to find their actual and virtual testing of this technology in each aspect of working condition. In this research article, a 2-dimensional model of four-bladed hydrokinetic savonius type turbine taken to investigate this performance and behaviour of the performance parameters of the turbine. A computational study has been carried out with the help of ANSYS codes.**

Keywords: ***Hydrokinetic, CFD, Fluid, Drag Force, Renewable Energy;***

I. INTRODUCTION

Renewable energy is a fast-growing energy need of world it has been observed over the two decades every country's governments finding the solution of every aspect of the green energy. They have been realized that global warming can destroy the worlds precious heritage. It should stop, as soon as possible, to use of fossil fuels. To achieve this, the government should take its steps to built a strong platform for policy and framework. There are lots of technologies are available to extract renewable energy according to the resources available. Some of them are matured enough to generate electricity within the great extents. However, there is a need to increase the efficiency of energy converters. Small hydro is one of them, which is still immature to commercialize compare to solar and wind energy converters. Providing predictable era, hydrokinetic electricity generation is an extra current shape of commercial renewable electricity, having a surprisingly excessive kinetic-energy density when water pace exceeds 2 m/s. Conventional hydropower technology extracts capability energy by using the elevation difference among two sides of boundaries or dams. Dams and limitations can have an ecological footprint. (El-Shamy, 1977)(Baxter, 1985)

Hydrokinetic mills extract power from ocean currents, ocean tides, and river currents without such structures. However, the lack of a structure introduces complexity to the preservation of the devices, and therefore impacts their reliability. (Birjandi, Woods, & Bibeau, 2012) Hydrokinetic strength technologies are highly new than different hydropower systems. In this work has been investigated these forms of hydrokinetic energy, and given a few exact information approximately modern-day base of hydrokinetic. It has attempted to offer a few know-how on the way to familiarize with the hydrokinetic turbine and generator.(Güney & Kaygusuz, 2010)(Khan, Bhuyan, Iqbal, & Quaicoe, 2009) Khan et. al presented Beginning with a fixed of basic definitions about this era, an overview of the present and upcoming conversion schemes, and their fields of programs are mentioned. Based on a complete survey of various hydrokinetic systems mentioned up to now, trendy traits in device design, duct augmentation, and site strategies are deduced. A particular evaluation of numerous turbine systems (horizontal and vertical axis), alongside their classification and qualitative comparison, is presented.

Ranges of experimental and numerical research with a massive number of physical designs and parameters have been done within the region of Savonius rotor to enhance its efficiency. Under this study, evaluate various parameters affecting the overall performance of the Savonius hydrokinetic turbine has been accomplished and offered on this paper which may be beneficial for future studies to enhance the performance of such mills.(Kumar & Saini, 2016). An experimental investigation along with computational fluid dynamics (CFD) study using Ansys 14.0 has been carried out to accomplish the objective of the work. To understand the significance of Savonius design in water application, the performance of the hydrokinetic turbine is experimentally compared to the identically designed wind turbine for the same input power values, showing enhanced performance of the former turbine. The purpose of using CFD is to enable a more detailed study on the velocity and torque distribution across the hydrokinetic turbine and hence to develop more insight into design information about its performance under low-velocity condition. Finally, the reason for the enhanced performance of the hydrokinetic turbine is investigated from the computational study of flow characteristics of both the hydrokinetic and wind turbines. (Sarma, Biswas, & Misra, 2014)

Experimental investigations are performed to take a look at the mutual interplay between mills with water because of the running medium at a Reynolds variety of 1.2 × 10 five based on the diameter of the turbine. Influence of separation hole between the two Savonius turbines is studied by way of various the separation hole ratio (X/R) from three to 8. As the separation hole ratio increases from three to 8, becomes lesser the mutual interaction between the mills. Results finish that generators positioned at a separation gap ratio of eight completed independently without affecting the overall performance of every different (Golecha, Eldho, & Prabhu, 2012). Every other study discovered with trying out of three open channels particularly small laboratory channel with a depth of water 270 mm, big laboratory channel with an intensity of water 480 mm and a real existence irrigation canal with an intensity of water 900 mm. Influence of endplates is studied to establish the significance in their presence on rotor overall performance. The maximum coefficient of power is located for an overlap ratio of round zero.11 for Savonius mills with factor ratio less than 0.6. For a given overlap ratio, the increasing fashion of the coefficient of energy is determined with the growth inside the aspect ratio. However, for aspect ratios extra than 1.8, the coefficient of electricity becomes nearly stagnant.(Patel, Bhat, Eldho, & Prabhu, 2017)

II. DESIGN OF ROTOR

A rotor of a savonius turbine has been considered for this study. A 2-Dimensional rotor with 4 bladed semicircular shapes is taken. A schematic of rotor geometry is shown in Figure 1. Rotor diameter is taken 1400 mm and the blade has a radius of 300 mm with a thickness of 10 mm. The gap between the blade tip and the rotation zone has taken about 50.27 mm. A shaft of radius 74.57 mm taken. AnotherFigure **1** describes the geometry of the fluid flow zone. A fluid zone is 9353.57 mm long and 2819.25 mm wide.

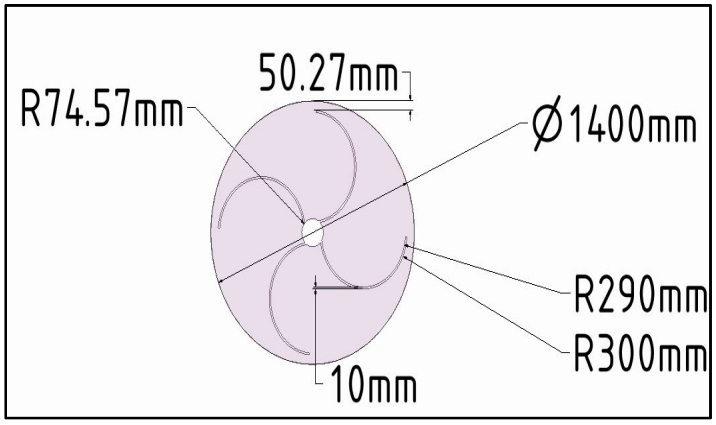

Figure 1: 2-dimensional savonius rotor with Rotation zone

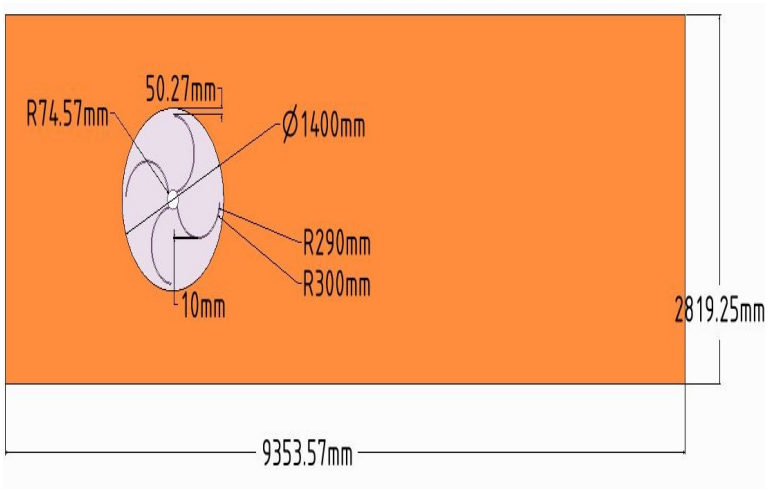

Figure 1: Fluid domain for flow analysis.

Length of the domain has to maintain the ratio of intake and outlet of 3d and 5d approximately. For the calculation purpose. Another rotation zone is provided for the turbine. However, for the sake of simplicity, a static model was studied.

III. THEORY AND PREPARATION

3.1. Mesh

For the whole computation zone, a single method of mesh adopted. Triangular /Quadrilateral multi zone method is selected for 2D meshing.

Table **1** is given below which describes the basic settings of the meshing. For 2D Study 71,955 nodes are considered with 0.005 element size. The number of elements is 70495, which is near to the number of nodes.

Table 1: Mesh Statics

Object Name	*Multi Zone Quad/Tri Method*
State	Fully Defined
Scope	
Scoping Method	Geometry Selection
Geometry	2 Bodies
Definition	
Suppressed	No
Method	Multi Zone Quad/Tri
Surface Mesh Method	Program Controlled
Element Order	Use Global Setting
Free Face Mesh Type	Quad/Tri
Advanced	
Preserve Boundaries	Protected
Mesh Based Disfeaturing	On
Disfeature Size	Default(2.4347e-003 m)
Sheet Loop Removal	No
Minimum Edge Length	2.9582e-003 m
Element Size	5.e-003 m
Nodes	71955
Elements	70495

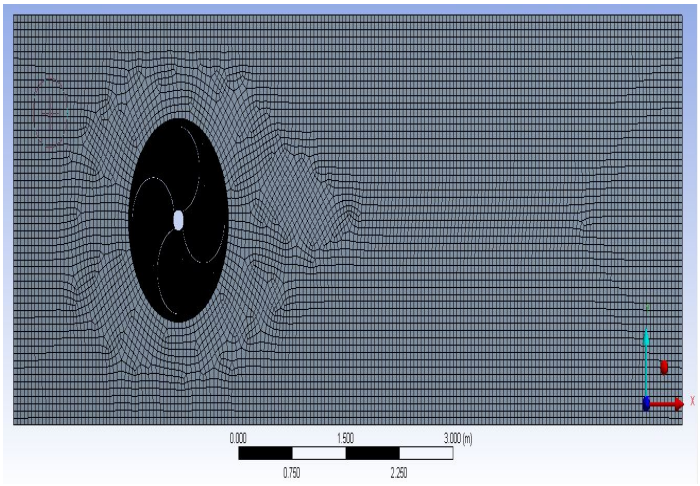

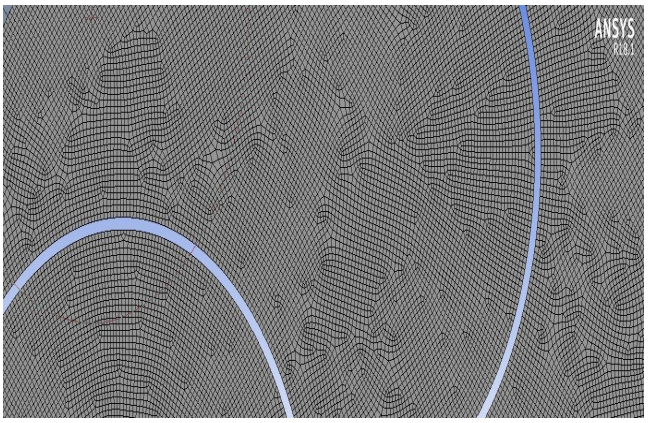

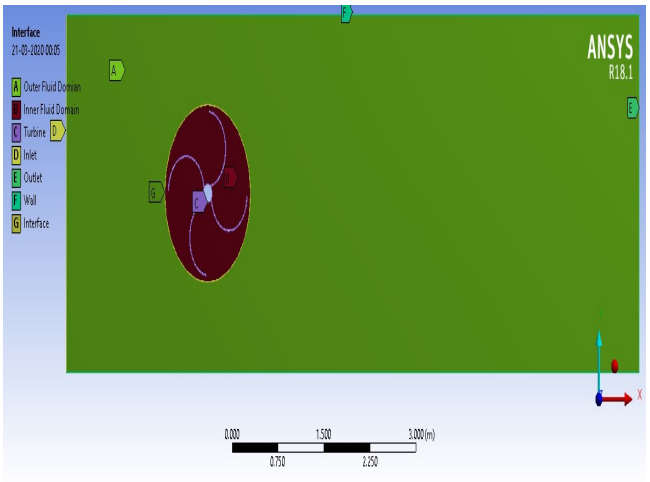

Figure 3: 2D mesh and zone named selection for rotor and domain

5.2. Numerical Modeling

In a Newtonian fluid, the relationship between the stress and the rate of deformation of the fluid is described by

$$\tau_{ij} = -P\delta_{ij} + \mu\left(\frac{\partial u_i}{\partial x_j} + \frac{\partial u_j}{\partial x_i}\right) + \delta_{ij}\,\lambda\frac{\partial u_i}{\partial x_i} \qquad (1)$$

Where:

τ_{ij} = stress tensor
U_i = orthogonal velocity
μ = dynamic Viscosity
λ = second coefficient

The final term, the product of the second coefficient of the viscosity and the divergence of the velocity, is zero, for constant density fluid and it is considered small enough to neglecting a compressible fluid.

Equation 1 transforms the momentum equations to the Navies –stokes equations: However, these will still be

referred to as the momentum equations elsewhere in this paper.
The momentum equation is as follows.

$$\frac{\partial \rho V_x}{\partial t} + \frac{\partial(\rho V_x V_x)}{\partial x} + \frac{\partial(\rho V_y V_x)}{\partial y} + \frac{\partial(\rho V_z V_x)}{\partial z} = \rho g_x - \frac{\partial P}{\partial x} + R_x + \frac{\partial}{\partial x}\left(\mu_e \frac{\partial V_x}{\partial x}\right) + \frac{\partial}{\partial y}\left(\mu_e \frac{\partial V_x}{\partial y}\right) + \frac{\partial}{\partial z}\left(\mu_e \frac{\partial V_x}{\partial z}\right) + T_x \quad (2)$$

$$\frac{\partial \rho V_y}{\partial t} + \frac{\partial(\rho V_x V_y)}{\partial x} + \frac{\partial(\rho V_y V_y)}{\partial y} + \frac{\partial(\rho V_z V_y)}{\partial z} = \rho g_y - \frac{\partial P}{\partial y} + R_y + \frac{\partial}{\partial x}\left(\mu_e \frac{\partial V_y}{\partial x}\right) + \frac{\partial}{\partial y}\left(\mu_e \frac{\partial V_y}{\partial y}\right) + \frac{\partial}{\partial z}\left(\mu_e \frac{\partial V_y}{\partial z}\right) + T_y \quad (3)$$

$$\frac{\partial \rho V_z}{\partial t} + \frac{\partial(\rho V_x V_z)}{\partial x} + \frac{\partial(\rho V)_y V_z)}{\partial y} + \frac{\partial(\rho V_z V_z)}{\partial z} = \rho g_z - \frac{\partial P}{\partial z} + R_x + \frac{\partial}{\partial x}\left(\mu_e \frac{\partial V_z}{\partial x}\right) + \frac{\partial}{\partial y}\left(\mu_e \frac{\partial V_z}{\partial y}\right) + \frac{\partial}{\partial z}\left(\mu_e \frac{\partial V_z}{\partial z}\right) + T_z \quad (4)$$

Where:\
gx,gy, gz =components of acceleration due to gravity.
ρ = Density
μe= Effective viscosity
Rx, Ry Rz = Distributed resistances
Tx, Ty, Tz = Viscous loss terms, Given below

$$T_x = \frac{\partial}{\partial x}\left(\mu \frac{\partial V_x}{\partial x}\right) + \frac{\partial}{\partial y}\left(\mu \frac{\partial V_y}{\partial x}\right) + \frac{\partial}{\partial z}\left(\mu \frac{\partial V_z}{\partial x}\right) \quad (5)$$

$$T_y = \frac{\partial}{\partial y}\left(\mu \frac{\partial V_x}{\partial y}\right) + \frac{\partial}{\partial y}\left(\mu \frac{\partial V_y}{\partial y}\right) + \frac{\partial}{\partial z}\left(\mu \frac{\partial V_z}{\partial y}\right) \quad (6)$$

$$T_z = \frac{\partial}{\partial x}\left(\mu \frac{\partial V_x}{\partial z}\right) + \frac{\partial}{\partial y}\left(\mu \frac{\partial V_y}{\partial z}\right) + \frac{\partial}{\partial z}\left(\mu \frac{\partial V_z}{\partial z}\right) \quad (7)$$

Turbulence means that the instantaneous velocity is fluctuating at every point in the flow field. The velocity is thus expressed in terms of a mean value and fluctuating components:

$$V_x = \overline{V}_x + V_x' \quad (8)$$

$\overline{V}_x$ = mean component of velocity in x-direction
V_x' = fluctuating component of velocity in x-direction

The dissipation rate equation is

$$\frac{\partial \rho \epsilon}{\partial t} + \frac{\partial(\rho V_x \epsilon)}{\partial x} + \frac{\partial(\rho V_y \epsilon)}{\partial y} + \frac{\partial(\rho V_z \epsilon)}{\partial z} = \frac{\partial}{\partial x}\left(\frac{\mu_t}{\sigma_\epsilon}\frac{\partial \epsilon}{\partial x}\right) + \frac{\partial}{\partial y}\left(\frac{\mu_t}{\sigma_\epsilon}\frac{\partial \epsilon}{\partial y}\right) + \frac{\partial}{\partial z}\left(\frac{\mu_t}{\sigma_\epsilon}\frac{\partial \epsilon}{\partial z}\right) + C_{1\epsilon}\mu_t \frac{\epsilon}{k}\Phi - C_2\rho\frac{\epsilon^2}{k} + \frac{C_\mu(1 - C_3)\beta\rho k}{\sigma_t}\left(g_x\frac{\partial T}{\partial x} + g_y\frac{\partial T}{\partial y} + g_z\frac{\partial T}{\partial z}\right)$$

The solution of turbulence equation is used to calculate the effective viscosity and the effective thermal conductivity
Where: μe =effective viscosity

$$\mu_e = \mu + C_\mu \rho \frac{k^2}{\epsilon} \quad (11)$$

k = Turbulent Kinetic Energy
ε = Turbulent kinetic energy dissipation rate

IV. COMPUTATION AND RESULT DISCUSSION

2-dimensional flow visualization has been identified for savonius rotor of 4 bladed semicircular. For this study a

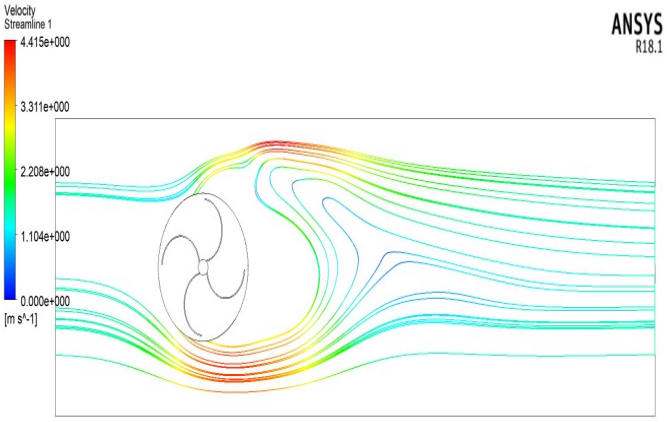

Figure 4: Distribution of streamlines for the velocity around the rotation zone.

a rectangular channel of dim 9353 x 2819 is considered. Figure 3 is showing the inlet, pressure outlet, interface wall, no-slip wall and tri/quad meshing cells. It has been observed that the streamlines are higher in number in -y-direction. However, the number isles in a +y direction. Due to the concave shape of the semicircular blade, more turbulence is created in +Y direction which leads to removal of streamlines in that region. It has been seen the maximum velocity found near the rotor.

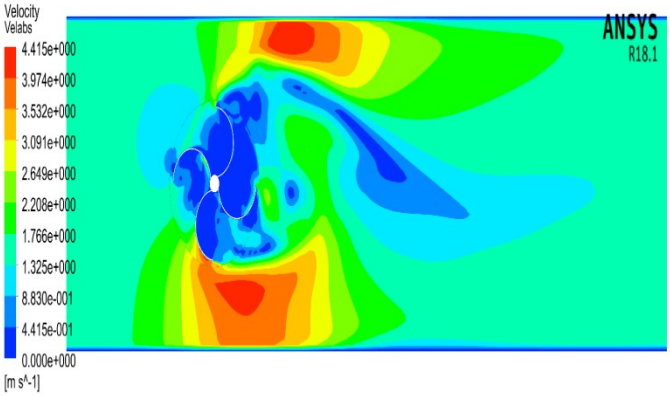

Figure 2: Absolute velocity V= Vx+Vy+Vz in the channel

Another absolute velocity for the channel flow around the savonius rotor is represented in Figure 2.there is no big difference in maximum velocity for this contour and x-direction velocity contour. However, Δmin for velocity is 1.98 m/s and it has been observed behind the rotor blades or opposite in direction of flow. Higher velocity zone is approximately similar to x-direction velocity irrespective its position. However, their various zone for the lower velocity has emerged for it. Velocity gets unaffected after distance ≈ 4D and before ≈ 1D from the rotor. A boundary layer can be seen near the no-slip wall boundary. Where velocity increases from nonslip to U_{∞}.

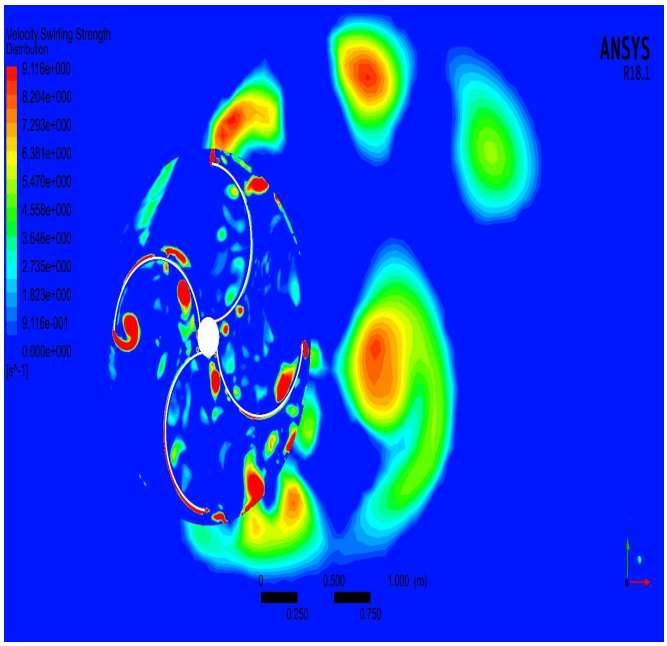

Figure 7: Swirl strength of the velocity

Swirl strength of the velocity would help to identify the negative and positive effect of the rotation of the rotor. Swirl generally reduces the energy available to generating the torque if the swirl is locally developed. Another side could be helpful for the rotor if it could generate globally.

Figure 7 showing the swirl strength for the channel flow around the rotor's blades. Here, it can be seen that the population of local swirl are more compared to lack of global swirl (which is global effects on each blade).

Local swirl flow strength decreases the axial velocity strength considerably, which is further leads to the performance of the rotor. As it can be seen all the swirls are developed near the rotor's blade and either of the sides. Some of the strong swirls have been emerged after the rotor and near the rotation zone. As it has been said earlier the swirls are killers of torque available for rotor blades.

Figure 8: Pressure distribution in the channel around the rotor

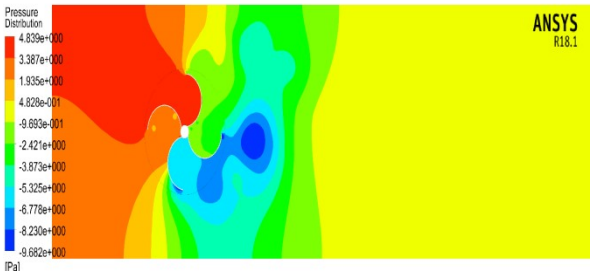

Pressure distribution for the flow is showing in Figure 8. Pressure distribution is well seen in the fluid flow zone highest pressure can be seen in the 2nd blade of the rotor. However, the lowest pressure can be seen near behind the 4th blade along the fluid flow direction. All four blades have different pressure contours. Pressure variations on the blades either sides are more in case of 2nd blade which is supportive for the torque requirements. It may be observed that the pressure contour after the distance ≈1.5D are similar for the remaining flow domain which tells that the low pressure is available for the rest of the flow domain which value is 0.4838 Pa. A blade 2nd has evidence of pressure value four times more than the atmosphere and at this pressure the impact of the water on the rotor's 2nd blade. On the other side of this same blade,the pressure is (-3.873 Pa)so total effective pressure on the blade is about four times of pressure outlet of the domain.

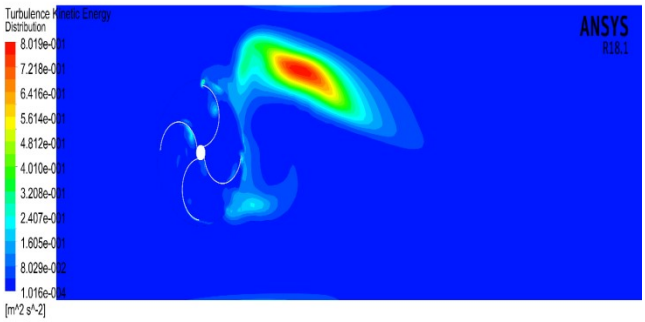

Figure 9: Contours of turbulence kinetic energy for the flow around available in the channel

A turbulence kinetic energy is a result of RANS application around the rotor and for a domain. Turbulence has been

created around the blades and rotor also, most of the times it has been created after the impact of the flow over the bluff body, above flow is just similar to the flow past over the bodies. In Figure 9 the turbulence kinetic energy in the domain is represented. The strong Turbulence kinetic energy zone established after the 2nd blade of the rotor this is due to the semicircular shape of the blade highly affects the impact of the water and separation of fluid starts at the leading edge of blades. However, fluid over the convex of the blade water slips easily on the blade 4th that helps to avoid the turbulence.

From the above discussion, the study of this 2D -4bladed rotor have been studied and found some interesting facts for the stationary flow

V. CONCLUSION

A savonius type 2D- 4 bladed rotors have been studied to investigate the flow around the rotor and behaviour of flow at the velocity of 0.5 m/s as an inlet. For this study, the 1st blade is 90° to the front of the flow. And blade 2nd found that bear lots of impact and drag over the flow of water. The highest value of pressure is found for the frontal side of the blade 2nd. Here is some observation which may be explained as follows.

1. Velocity in the x-direction is highly affected the wall shear and it is greatly affected the distribution of x-direction velocity.
2. The swirl velocity strength is largely distributed near the blade zone or higher in the number of local distribution of it. There is a lack of distribution of global velocity swirl.
3. The total pressure has mostly impinged on the 2nd blade of the rotor. Which is positive for torque generation?
4. The turbulence intensity is weak in between the rotor blades. However, stronger at nearer to the blades and after to the blades.

There is a lot of work has to be done for this type of rotors such as parametric studies over the angle and shape modification. A full-body model study has been suggested to investigate its performance over different surface velocities.

ACKNOWLEDGEMENTS

The authors are thankful to the Rama University, Kanpur and ABES Engineering College, Ghaziabad who support for this study. Authors also thanks to MNRE for their inspiration towards renewable energy development.

REFERENCES

[1] Baxter, R. M. (1985). Environmental effects of reservoirs. *Microbial Processes in Reservoirs*. https://doi.org/10.1007/978-94-009-5514-1_1

[2] Birjandi, A. H., Woods, J., & Bibeau, E. L. (2012). Investigation of macro-turbulent flow structures interaction with a vertical hydrokinetic river turbine. *Renewable Energy*, *48*, 183–192. https://doi.org/10.1016/j.renene.2012.04.045

[3] El-Shamy, F. M. (1977). ENVIRONMENTAL IMPACTS OF HYDROELECTRIC POWER PLANTS. *ASCE J Hydraul Div*.

[4] Golecha, K., Eldho, T. I., & Prabhu, S. V. (2012). Study on the interaction between two hydrokinetic Savonius turbines. *International Journal of Rotating Machinery*, *2012*. https://doi.org/10.1155/2012/581658

[5] Güney, M. S., & Kaygusuz, K. (2010). Hydrokinetic energy conversion systems: A technology status review. *Renewable and Sustainable Energy Reviews*, *14*(9), 2996–3004. https://doi.org/10.1016/j.rser.2010.06.016

[6] Khan, M. J., Bhuyan, G., Iqbal, M. T., & Quaicoe, J. E. (2009). Hydrokinetic energy conversion systems and assessment of horizontal and vertical axis turbines for river and tidal applications: A technology status review. *Applied Energy*, *86*(10), 1823–1835. https://doi.org/10.1016/j.apenergy.2009.02.017

[7] Kumar, A., & Saini, R. P. (2016). Performance parameters of Savonius type hydrokinetic turbine - A Review. *Renewable and Sustainable Energy Reviews*. https://doi.org/10.1016/j.rser.2016.06.005

[8] Patel, V., Bhat, G., Eldho, T. I., & Prabhu, S. V. (2017). Influence of overlap ratio and aspect ratio on the performance of Savonius hydrokinetic turbine. *International Journal of Energy Research*. https://doi.org/10.1002/er.3670

[9] Sarma, N. K., Biswas, A., & Misra, R. D. (2014). Experimental and computational evaluation of Savonius hydrokinetic turbine for low velocity condition with comparison to Savonius wind turbine at the same input power. *Energy Conversion and Management*. https://doi.org/10.1016/j.enconman.2014.03.070